General Disclaimer

One or more of the Following Statements may affect this Document

- This document has been reproduced from the best copy furnished by the organizational source. It is being released in the interest of making available as much information as possible.

- This document may contain data, which exceeds the sheet parameters. It was furnished in this condition by the organizational source and is the best copy available.

- This document may contain tone-on-tone or color graphs, charts and/or pictures, which have been reproduced in black and white.

- This document is paginated as submitted by the original source.

- Portions of this document are not fully legible due to the historical nature of some of the material. However, it is the best reproduction available from the original submission.

X-682-77-7

PREPRINT

TMX 71260

THE HIGH ENERGY X-RAY SPECTRUM OF THE CRAB NEBULA OBSERVED FROM OSO 8

J. F. DOLAN
C. J. CRANNELL
B. R. DENNIS
L. E. ORWIG
G. S. MAURER
K. J. FROST

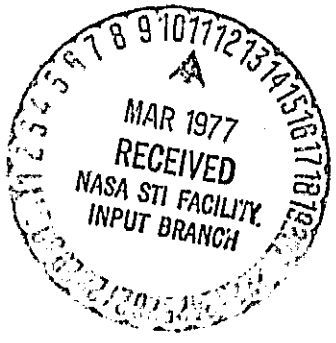

JANUARY 1977

GSFC — GODDARD SPACE FLIGHT CENTER —
GREENBELT, MARYLAND

THE HIGH ENERGY X-RAY SPECTRUM OF THE CRAB NEBULA OBSERVED FROM OSO 8

J. F. Dolan[+], C. J. Crannell, B. R. Dennis, L. E. Orwig, G. S. Maurer* and K. J. Frost

Laboratory for Solar Physics and Astrophysics

NASA - Goddard Space Flight Center

Greenbelt, Maryland

January, 1977

+ NAS-NRC Senior Resident Research Associate

* Also Department of Physics, Catholic University of America. Work done in partial fulfillment of requirements for Ph. D. degree.

ABSTRACT

The X-Ray spectrum of the Crab Nebula was measured with the scintillation spectrometer on board the OSO-8 satellite between 1976 March 9 and 23. The spectrum is well fitted from 23 to 513 keV by a power law of the form $dN/dE = C(E/E_o)^{-\alpha}$ photons $cm^{-2}s^{-1}keV^{-1}$ with $C = (4.19 \pm 0.18) \times 10^{-3}$ photons $cm^{-2}s^{-1}keV^{-1}$, $E_o = 39.1$ keV, and $\alpha = 2.00 \pm 0.08$. No indication is found of either day-to-day or long term variability in the time averaged X-ray spectrum of the source.

I. INTRODUCTION

The X-ray spectrum of the Crab Nebula has been measured many times in the past 12 years and considerable evidence has been accumulated indicating that the intensity has not changed significantly during that time (Toor & Seward 1974). The spectrum is well represented by a single power low over a wide energy range. However, there still exists some uncertainty about the constancy of the source and the exact shape of the spectrum at higher energies (greater than 20 keV). In the past, most of the observations at these higher energies have been made from balloon-borne instruments. Systematic uncertainties associated with calculations of the absorption by the overlying atmosphere have left the measured spectrum open to question. In this paper we present the results of an observation of the Crab Nebula from a satellite. The measured spectrum extends from 20 to 500 keV with lower statistical and systematic uncertainties than have been achieved previously in this energy range.

The Crab Nebula X-ray source and its associated pulsar, NP0532, were observed between 1976 March 9 and 1976 March 23 with the high energy X-ray spectrometer on board the OSO-8 satellite, which was launched 1975 June 21 into Earth orbit. One of the experiments in the rotating wheel section of the satellite is a CsI(Na) crystal scintillation detector used with an associated 256 channel pulse height analyzer as an X-ray spectrometer. The choice of electronic gains available on command from the ground allows the analysis of incident spectra between photon energies of 20 keV and 3 MeV. A cross-sectional view of the instrument is shown in Figure 1. The sensitive area of the detector is

27.5 cm^2 and it is actively collimated with additional CsI shielding, which provides a circular field of view of 5.1 degrees FWHM. A second, identical crystal, mounted beside the first but completely shielded, serves as a monitor of the spectrum of the internal background of the detector. The instrument is mounted with the axis of its field of view offset by 5 degrees from the (negative) spin axis of the rotating wheel as indicated in Figure 2. Once every 10 seconds, the period of rotation of the wheel, a source positioned 5 degrees from the spin axis will pass through the center of the field of view. The measured energy resolution of the detector is well represented by FWHM = 1.45 $E^{0.7}$ keV, where FWHM is the full width at half-maximum, in keV, of a monochromatic line at E keV. This gives an energy resolution (FWHM/E) of 21% at 662 keV, and 36% at 100 keV. For a complete description of the instrument and its operation on board the spacecraft, see Dennis et al. (1977).

Because of the pointing requirements of the spacecraft, the spin axis is constrained to precess around the sky once every year, always lying within 4 degrees of a great circle, one pole of which is the direction to the sun. The resultant geometry allows observations of any source near the ecliptic for a maximum duration of 18 days. The results described here are based on observations made 1976 March 8.94 UT to 10.73 UT and 1976 March 17.21 UT to 23.96 UT.

II. ANALYSIS OF THE DATA

In order to determine the strength of a point source detected in the presence of both cosmic and instrumental background, we make use of

the spinning motion of the spacecraft and the resultant modulation of the signal from the source. As the spacecraft spins, the look-axis of the detector describes a small circle of half angle 5° on the celestial sphere. The detector area projected in the direction of the point source, relative to the sensitive area of the collimated detector, varies between zero and unity for a source located on the scan circle. The data for a particular energy interval are analyzed by sorting the events into intervals corresponding to the angular separation between the look-axis of the detector and the vector from the detector to the point source at the time of the detected event (see Figure 3). Any variations in the detector background on a time scale long compared to the 10 second satellite rotation period will affect all angular intervals equally.

The sum of the cosmic plus instrumental background is determined each satellite orbit from the mean counting rate when no source is in the field of view. The observed source strength is determined each orbit from a weighted least-squares fit of the observed counting rate to the calculated angular response function of the detector. The source strength for orbit p is given by

$$S(p) = \frac{\sum_{|j| \leq J} \frac{\left[N(j,p) - B(j,p)\right] t(j,p) F(j)}{\left[\sigma_N^2(j,p) + \sigma_B^2(j,p)\right]}}{\sum_{|j| \leq J} \frac{\left[t(j,p) F(j)\right]^2}{\left[\sigma_N^2(j,p) + \sigma_B^2(j,p)\right]}}, \quad (1)$$

where $N(j,p)$ is the total number of counts observed in angular interval j during orbit p;

$B(j,p)$ is the number of background counts expected in interval j during orbit p;

$t(j,p)$ is the live time in interval j during orbit p;

$F(j)$ is the effective source sensitivity of the detector (i.e., the ratio of the effective area the detector presents to the source to its geometric area) in angular interval j;

$\sigma_N(j,p)$ is the one-sigma uncertainty in $N(j,p)$; and

$\sigma_B(j,p)$ is the one-sigma uncertainty in $B(j,p)$.

The index j runs from -J to J, over all those angular bins for which $F(j)$ in non-zero. The corresponding uncertainty in the observed source strength is determined from the variance in the measurements and is given by

$$\delta S(p) = \left\{ \frac{\sum_{|j| \le J} \frac{\left[N(j,p) - B(j,p) - t(j,p)\ F(j)\ S(p) \right]^2}{\left[\sigma_N^2(j,p) + \sigma_B^2(j,p) \right]}}{2J-1 \sum_{|j| \le J} \frac{\left[t(j,p)\ F(j) \right]^2}{\left[\sigma_N^2(j,p) + \sigma_B^2(j,p) \right]}} \right\}^{\frac{1}{2}} . \quad (2)$$

If $t(j,p)$ and $F(j)$ are in units of seconds and fractional area, respectively, then $S(p)$ and $\delta S(p)$ are in units of counts per second. The source strength is determined from an extended period of observation by a

weighted mean of the individual, orbit-by-orbit strengths. For a total of P orbits the source strength and corresponding uncertainty are given by

$$S = \frac{\sum_{p=1}^{P} \frac{S(p)}{\left[\delta S(p)\right]^2}}{\sum_{p=1}^{P} \frac{1}{\left[\delta S(p)\right]^2}}, \tag{3}$$

and

$$\delta S = \frac{1}{\left\{\sum_{p=1}^{P} \frac{1}{\left[\delta S(p)\right]^2}\right\}^{\frac{1}{2}}}, \tag{4}$$

or

$$\delta S = \left\{ \frac{\sum_{p=1}^{P} \frac{\left[S - S(p)\right]^2}{\left[\delta S(p)\right]^2}}{(P-1)\sum_{p=1}^{P} \frac{1}{\left[\delta S(p)\right]^2}} \right\}^{\frac{1}{2}}. \tag{5}$$

The expected statistical uncetainty in S, Equation (4), and the observed standard deviation, Equation (5), are compared. For the quoted uncertainty in the source strength, we use the larger of the two estimates, Equation (4) or (5).

The counting rate in the detector produced by the source is reduced to the incident spectrum by the matrix inversion scheme described by Dolan (1972). The effect of the finite energy resolution of the detector is removed by apodization; and then the effects of fluorescent escape photons, detector quantum efficiency, and absorption in overlying material are removed by using the measured properties of the detector obtained during laboratory calibration. The data are analyzed in energy bins of bandwidth approximately one standard deviation (0.424 FWHM) of the energy resolution of the detector. During the observations described in this paper, bins 10 keV wide were used between 23 and 123 keV, and bins 30 keV wide between 123 and 783 keV. After the completion of this reduction procedure, the resultant incident fluxes derived for adjacent bins may be combined to produce an average intensity in a wider energy bandwidth which is statistically more significant. The incident spectrum so derived is then compared directly with the intensity predicted by any assumed source mechanism to determine whether any simple set of spectral parameters is consistent with the data.

III. RESULTS

The spectrum derived from our observations is shown in Figure 4. It is the time-averaged spectrum of the Crab Nebula over the duration

of our observations and, as such, includes the average intensity of the X-ray pulsar, NP 0532. The spectrum of the pulsar alone and the fraction of the total radiation it contributes is the subject of a separate paper (Maurer et al 1977). The photon spectrum in Figure 4 is well fitted ($\chi^2 = 4.24$ for 8 degrees of freedom) by a power law of form $dN/dE = C(E/E_o)^{-\alpha}$ photons cm^{-2} s^{-1} keV^{-1}, with $C = (4.19 \pm 0.18) \times 10^{-3}$ photons $cm^{-2}s^{-1}$ keV^{-1}, $E_o = 39.1$ keV, and $\alpha = 2.00 \pm 0.08$. A plot of χ^2 in (C, α) parameter space is shown in Figure 5. The contours of equal probability (equal χ^2) are approximately elliptical with axes parallel to the C and α axes, showing that the uncertainties in C and α are nearly independent. This results from expressing the energy in units of the weighted logarithmic mean energy, E_o, of our total bandwidth. Then σ_α refers only to the slope of the line pivoting about the point fixed in intensity at E_o, and σ_C refers only to the intensity at E_o of the line moving up and down with fixed slope α.

Comparison of the spectra derived from individual, one-day observations with the average spectrum of the Crab in Figure 4 reveals no evidence for day-to-day variations in the spectrum of the source. The χ^2 test shows each individual spectrum is compatible, within its statistical accuracy, with the spectrum given above.

IV. DISCUSSION

Toor and Seward (1974) discuss the observations published before 1973 of the Crab Nebula X-ray spectrum between 2 and 200 keV. They conclude that the total emission of the source is steady over a time

scale of years, and that the spectrum of the Crab Nebula is a power law in energy with spectral index unchanging over a wide bandwidth. Toor and Seward recommend adoption of a power law photon spectrum with $\alpha = -2.08 \pm 0.05$ between 2 and 100 keV. Our spectrum is consistent with this, and is evidence for the single power-law character of the Crab Nebula spectrum out to at least 200 keV and probably to as high an energy as 500 keV. We note in passing that the intensity (E dN/dE) we measure at 40 keV is (0.160 ± 0.007) keV cm^{-2} s^{-1} keV^{-1}, consistent with the constant intensity hypothesis presented in Figure 2 of Toor and Seward.

Toor and Seward discuss several observations discordant with the constant source hypothesis, and conclude that observations from balloons may have large systematic uncertainties of up to 50% in the observed intensities. Laros et al. (1973) present a balloon-borne observation not discussed by Toor and Seward which is also discordant with the constant source hypothesis. They fit their spectrum of the total emission observed on two days in 1970 September by a power law of slope $\alpha = 2.29 \pm 0.06$ between 25 and 150 keV. Further, they observe a break in the spectral index at 150 keV; their best fit spectral index between 60 and 300 keV is $\alpha = 2.46 \pm 0.11$. We see no evidence for their reported drop in intensity above 150 keV. Although their fitted spectrum has an intensity everywhere close to the one we observe, except at our lowest energies, the slope of their spectrum is not compatible with ours. Laros et al. see the drop in intensity above 150 keV as being almost entirely in the steady emission, and not the pulsar spectrum. The majority of the flux from the Crab Nebula is from the extended source and not the pulsar.

It is difficult to understand how the emission could change significantly on time scales shorter than 2 years, since the approximate diameter of the emitting region at these energies is 2 light years (Ku et al. 1976). If we are to accept the constancy of the Crab Nebula spectrum, this discordant observation must be regarded as indicative of some unknown systematic error.

The reported variations in the spectrum of the Crab Nebula from balloon-borne observations emphasize the improtance of measurements from satellites, where the problem of correcting for the absorption in the overlying atmosphere is not present. The only other satellite measurements at energies of 60 keV and above were reported by Schwartz (1969) and Carpenter et al. (1975). Their observed spectra are in agreement with ours. It must be pointed out, however, that the analysis of the data obtained by Carpenter et al may contain systematic uncertainties caused by the unknown thickness of the crystal dead layer on their Cs I detector (cf. Goodman 1975) as well as by the apparent modulation of the background they observe with their satellite's rotation.

If a single power law spectrum with an index of -2.0 to -2.1 is assumed for the Crab Nebula up to energies on the order of 500 keV, then significant changes must be made in various models of the Nebula. Cocke (1975) assumes a power law index of -2.3 at energies above 0.1 keV. He concludes from the extrapolation of this spectrum to lower energies and from the radio, infrared, and ultraviolet observations that there must be two breaks in the electromagnetic spectrum - one at 3×10^{14} Hz and a second at 3×10^{16} Hz. The X-ray spectrum with a slope of -2.08 extrapolated

back in frequency shows that only one break is needed, at $\approx 10^{14}$Hz. This break is usually interpreted as resulting from the transition between synchrotron losses at low energies and electron escape from the Nebula at high energies. The break at 10^{14}Hz also means that the electron injection energy for the pulsar into the Nebula can be characterized by a Lorentz factor $\gamma = 7 \times 10^5$, in agreement with analytical calculations cited by Cocke.

Weinberg and Silk (1976) also have compared the predictions of their model to a power law spectrum with an index of -2.3. They conclude that a break in the spectrum occurs at 2×10^{15}Hz and that most of the X-rays above 1 keV are from the injection region rather than from the Nebula itself. Their model also predicts a turn-over in the spectrum above 100 keV, which is suggested by the data of Laros et al. (1973) but not supported by our data nor by the data of Carpenter et al. (1976).

V. CONCLUSIONS

We conclude, with Toor and Seward, that the total emission of the Crab Nebula X-ray source shows no long term variability, and that the X-ray spectrum itself can be described by a single power law out to energies of at least 500 keV.

Acknowledgements

We acknowledge the efforts of the many people who made this observation possible: the personnel in the Laboratory for Solar Physics and Astrophysics, project scientist Roger J. Thomas in particular, and the OSO Project office and control center. In addition, we thank the personnel of COMTECH Inc., Edwin P. Cutler in particular, for assistance with the data analysis.

REFERENCES

Carpenter, G. F., Coe, M. J., and Engel, A. R. 1976, Nature, 259, 99.

Cocke, W. J. 1975, Ap. J., 202, 773.

Dennis, B. R., Frost, K. J., Lencho, R. J., and Orwig, L. E., 1977, Space Sci. Instr., in press.

Dolan, J. F. 1972, Ap. and Space Sci., 17, 472.

Goodman, N. 1976, Space Sci. Instr., in press.

Ku, W., Kestenbaum, H. L., Novick, R., and Wolff, R. S. 1976, Ap. J. (Letters), 204, L77.

Lampton, M., Margon, B., and Bowyer, S. 1976, Ap. J., 208, 177.

Laros, J. G., Matteson, J. L., and Pelling, R. M. 1973, Nature (Phys. Sci.), 246, 109.

Maurer, G. S., Orwig, L. E., Crannell, C. J., Dennis, B. R., Dolan, J. F., and Frost, K. J. 1977, in preparation.

Schwartz, D. A. 1969, Unpublished Ph. D. thesis, University of Calif. at San Diego

Toor, A., and Seward, F. D. 1974, A. J., 79, 995.

Weinberg, S. L., and Silk, J. 1976, Ap. J., 205, 563.

C. J. CRANNELL, B. R. DENNIS, J. F. DOLAN, K. J. FROST, G. S. MAURER AND L. E. ORWIG: Code 682, NASA - Goddard Space Flight Center, Greenbelt, Maryland 20771

FIGURE CAPTIONS

Figure 1. The OSO-8 high energy spectrometer. The detector has 27.5 cm^2 sensitive area, $5^\circ.1$ FWHM circular collimation, and a sensitive area X solid angle factor of 0.25 cm^2 sr.

Figure 2. A schematic outline of the experiments on board the OSO-8 spacecraft. The high energy X-ray spectrometer is mounted in the wheel with the axis of its field of view offset by 5 degrees from the negative spin axis.

Figure 3. The counting rate in the energy interval 25 to 100 keV as a function of the angular separation between the axis of the detector field of view and the source. The data shown were obtained for one day of observation of the Crab Nebula. The counting rate in each bin is the weighted mean of the difference between the observed rate and the mean background rate determined each individual orbit (96 minutes duration) during that day's observations. Negative angular distances correspond to that side of the source when the detector look axis was approaching; positive when receding.

Figure 4. The photon spectrum of the Crab Nebula observed between 1976 March 9 and March 23. The uncertainties on each point are $\pm$ one standard deviation mean error in the count rates as propagated through the reduction procedure. The straight line is the power law spectrum suggested by Toor and Seward (1974) as the spectral shape between 2 and 100 keV, with $C = 9.5(\pm 1.0)$, $E_o = 1$ keV, and $\alpha = 2.08(\pm 0.05)$.

Figure 5. A plot of equal χ^2 probability contours in (C, α) parameter space. Minimum χ^2 (4.24) is obtained for C = 4.19×10^{-3} photons cm^{-2} s^{-1} keV^{-1} and $\alpha = 2.00$. The probability, P, of the residuals being exceeded by random deviations equals 0.80. The contours drawn for 8 degrees of freedom correspond to a decrease in P to 0.32 and 0.045, equivalent to a one and two standard deviation error in the parameters, respectively (Lampton et al. 1976).

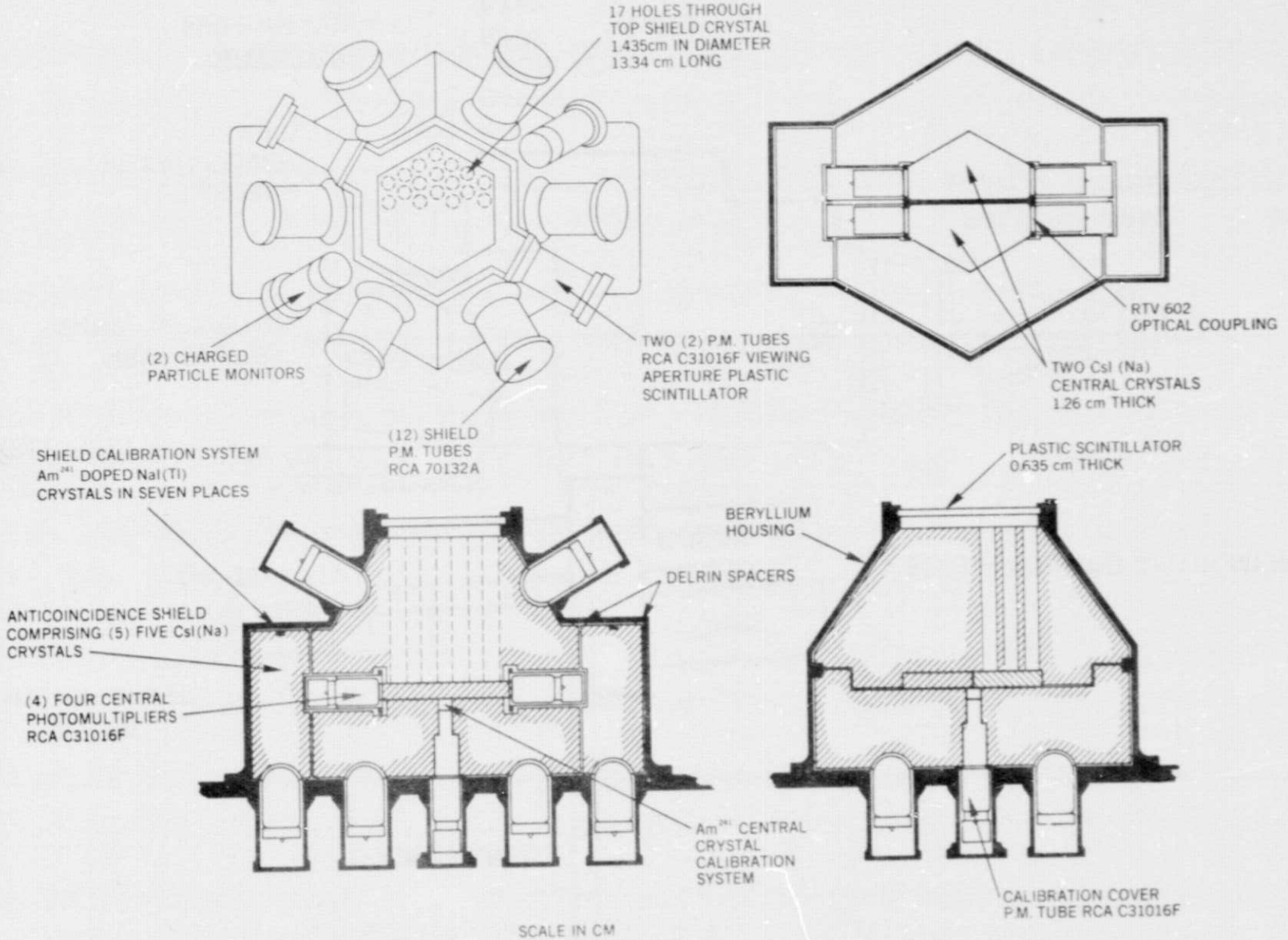

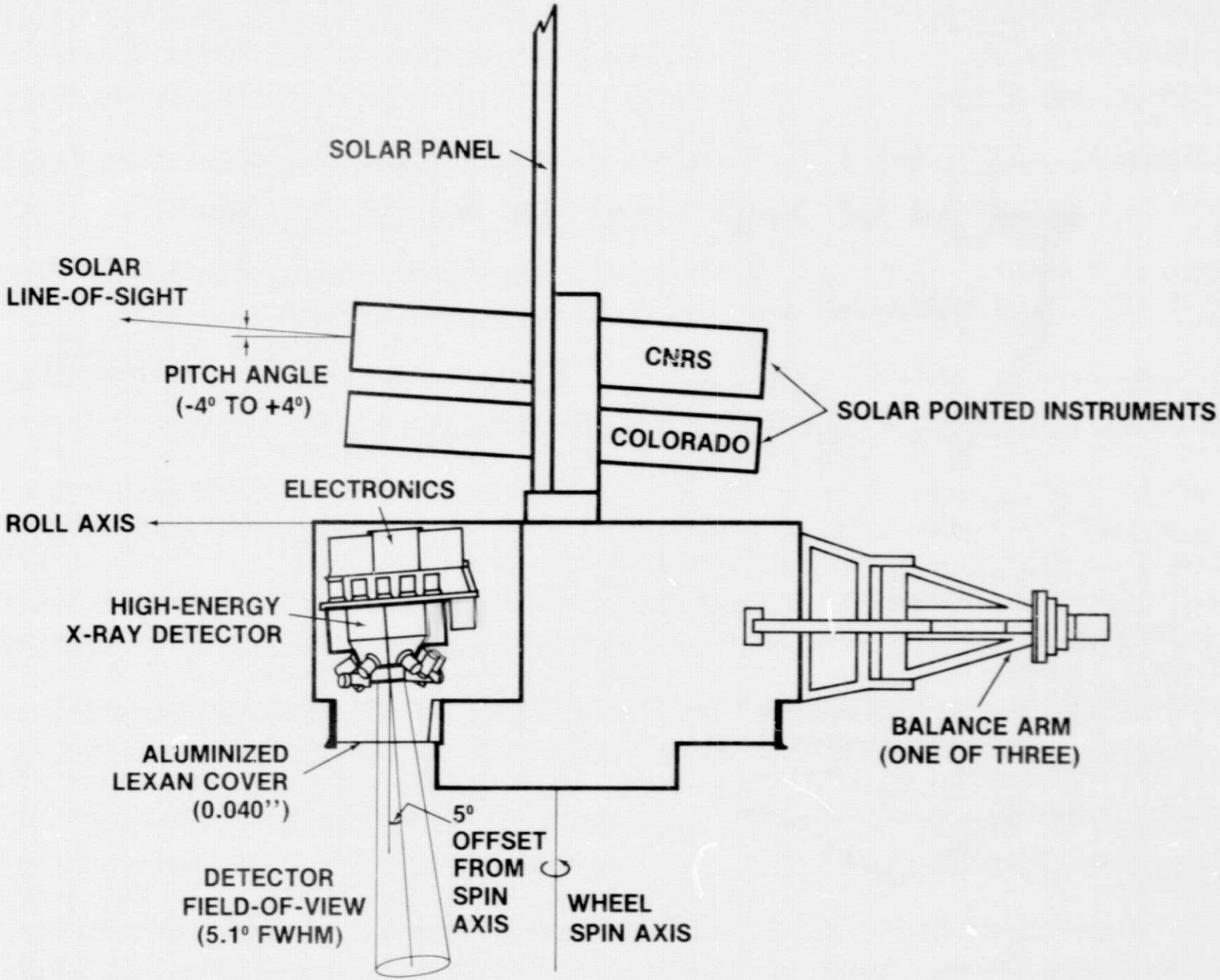
SOLAR PANEL
SOLAR
LINE-OF-SIGHT
PITCH ANGLE
(-4° TO +4°)
CNRS
COLORADO
SOLAR POINTED INSTRUMENTS
ELECTRONICS
ROLL AXIS
HIGH-ENERGY
X-RAY DETECTOR
BALANCE ARM
(ONE OF THREE)
ALUMINIZED
LEXAN COVER
(0.040'')
5°
OFFSET
FROM
SPIN
AXIS
DETECTOR
FIELD-OF-VIEW
(5.1° FWHM)
WHEEL
SPIN AXIS

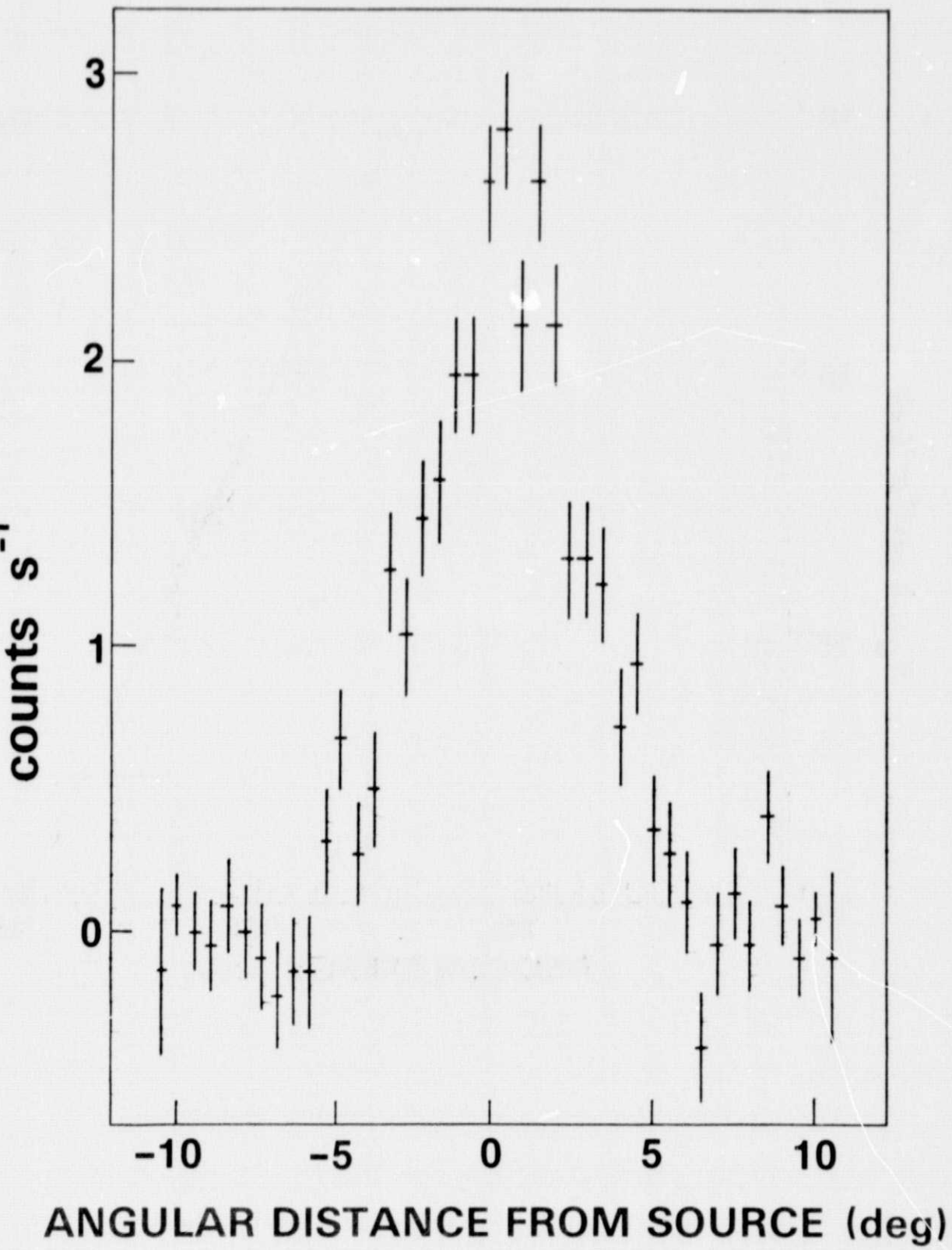
3
2
1
0
counts s^{-1}
−10
−5
0
5
10
ANGULAR DISTANCE FROM SOURCE (deg)

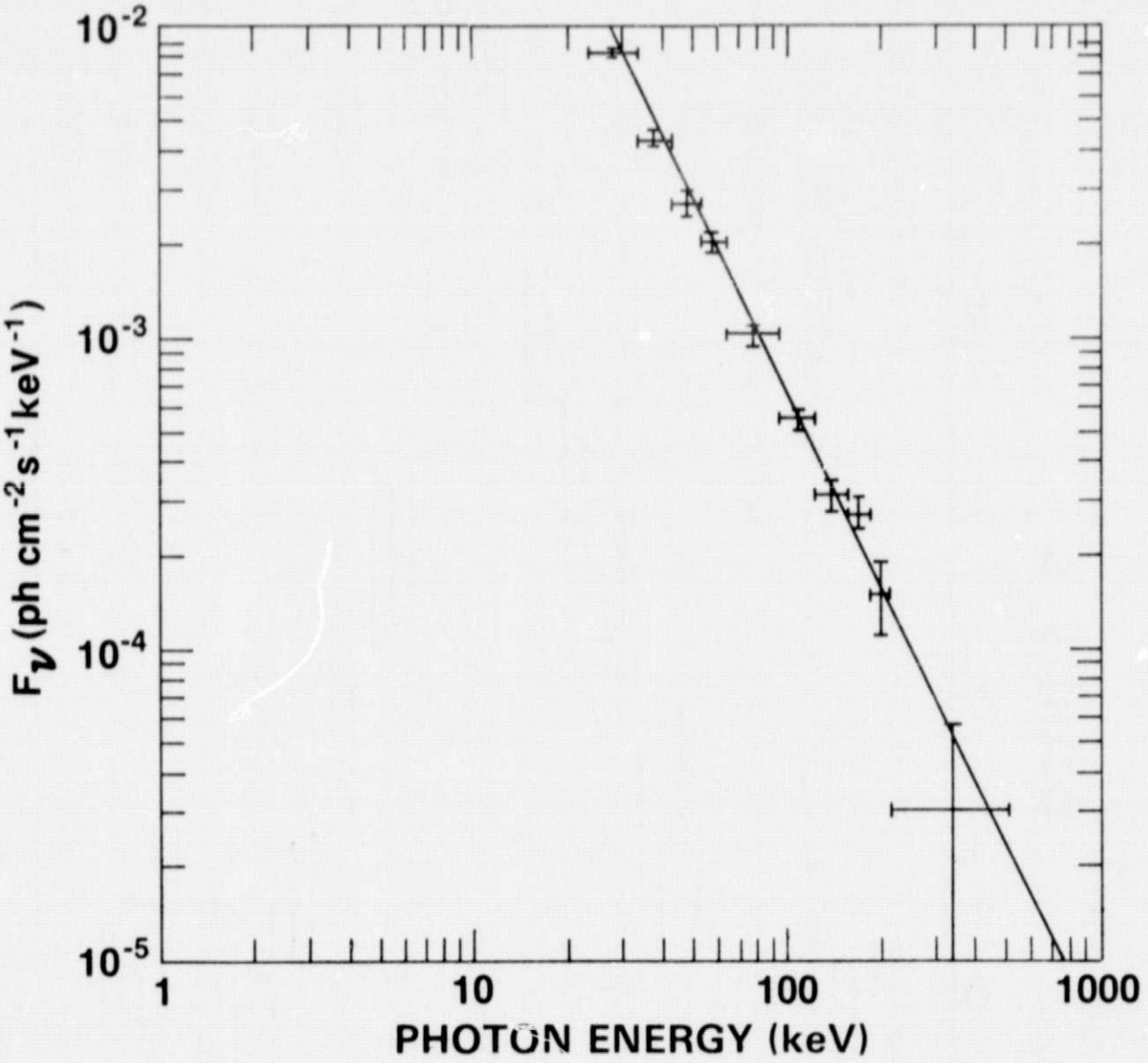
10^{-2}
10^{-3}
10^{-4}
10^{-5}
F_ν (ph cm^{-2} s^{-1} keV^{-1})
1
10
100
1000
PHOTON ENERGY (keV)

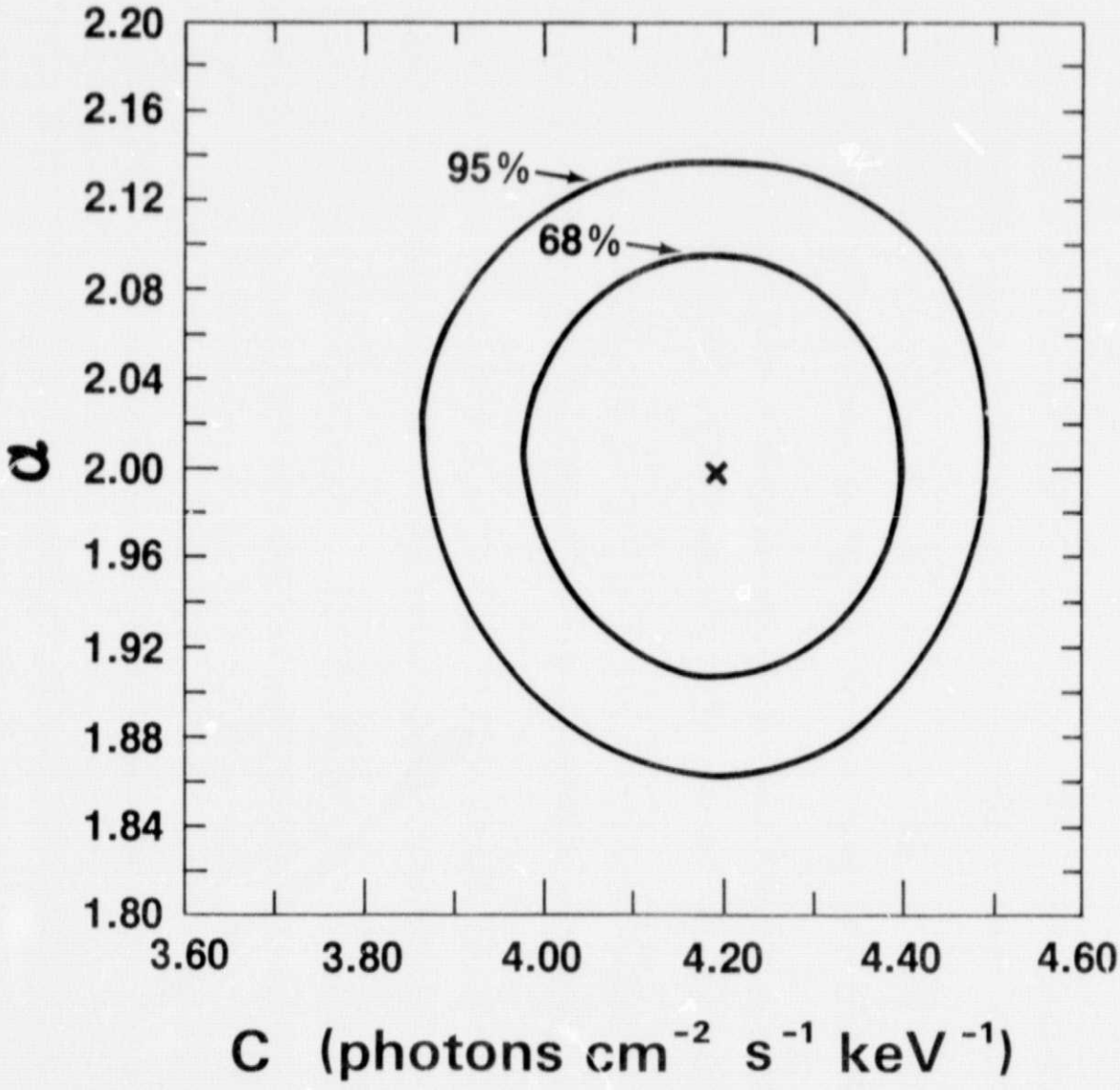
2.20
2.16
2.12
2.08
2.04
2.00
1.96
1.92
1.88
1.84
1.80
α
95%
68%
3.60
3.80
4.00
4.20
4.40
4.60
C (photons cm^{-2} s^{-1} keV^{-1})